Ultrahigh-Resolution Optical Coherence Tomography with LED-Phosphor-Based Broadband Light Source

2013 Appl. Phys. Express 6 122502

(http://iopscience.iop.org/1882-0786/6/12/122502)

Applied Physics Express 6 (2013) 122502
http://dx.doi.org/10.7567/APEX.6.122502

Ultrahigh-Resolution Optical Coherence Tomography with LED-Phosphor-Based Broadband Light Source

Meng-Tsan Tsai[1], Jeng-Jie Hung[2], and Ming-Che Chan[2]*

[1]*Department of Electrical Engineering, Chang Gung University, Kweishan, Taoyuan 33302, Taiwan*
[2]*Institute of Imaging and Biomedical Photonics, College of Photonics, National Chiao-Tung University, Hsinchu 300, Taiwan*
E-mail: mcchan@nctu.edu.tw

Received September 3, 2013; accepted November 4, 2013; published online November 19, 2013

This study proposed and demonstrated the potential use of LED phosphors as a simple light source for ultrahigh-resolution spectral-domain optical coherence tomography (SD-OCT) in the visible regime. Excited by a 405 nm diode laser, broadband spontaneous emission from three different LED phosphors was generated. The best axial resolution was 1.7 μm in air, and finally, corresponding three-dimensional (3D) ultrahigh-resolution SD-OCT imaging was performed with the proposed broadband light source.

Optical coherence tomography (OCT), which is inherently a low-coherence interferometer, enables three-dimensional (3D) noninvasive biopsy of partially transparent samples.[1)] For future OCT applications, the imaging acquisition speed[2)] and resolution[3)] are two key issues. The imaging speed is determined by the scanning mechanism. In a time-domain OCT (TD-OCT) system, to acquire a depth profile (A-scan), the length of the reference arm has to be mechanically changed, which limits the imaging speed. Recently, advanced by Fourier-domain OCT (FD-OCT) including swept-source OCT (SS-OCT)[4,5)] and spectral-domain OCT (SD-OCT),[6)] the imaging speed has been greatly improved to hundreds of frames per second by the removal of mechanical scanners in the reference arm. Furthermore, FD-OCT shows superior imaging speed and system sensitivity than those of TD-OCT systems.[6)] In SS-OCT systems, a MEMS-based swept source or a Fourier domain mode-locked laser can provide an A-scan rate of more than 100 kHz,[4,5)] enabling motion artifacts during OCT scanning to be greatly reduced. In contrast, the imaging speed of SD-OCT system is determined by a high-speed line-scan CCD, which is employed as a detection mechanism. Currently, commercial line-scan CCDs can achieve a line rate of ~100 kHz, equal to the A-scan rate of the SD-OCT system. Thus, either SS-OCT or SD-OCT systems are capable of providing a higher imaging speed than TD-OCT.

The other key issue of the OCT system is the image resolution. In the OCT system, the transverse resolution is determined by the focus lens used in the sample arm, and the longitudinal resolution is inversely proportional to the bandwidth of the light source. Recently, to achieve a high longitudinal resolution in OCT systems, various broadband light sources have been demonstrated including supercontinuum generation (SCG) of femtosecond laser pulses in highly nonlinear fibers,[7,8)] superluminescent diode (SLD),[9)] halogen lamps,[10)] and crystal fibers.[3,11)] SCG sources can provide sub-μm axial resolution in OCT systems. However, SCG sources are not cost effective and with high amplitude noises. In contrast, multiple-quantum-well SLD-based sources are compact, highly reliable, and with a low operation difficulty. However, it is not easy and straightforward to design ultra-broadband SLDs by combining multiple SLDs.[9)] The lamp is intrinsically a low-cost broadband source, but the low power density and thermal problem are two major drawbacks.[10)] Crystal-fibers-based light sources delivered ultra-broadband Gaussian-like spectra. 1.5-μm-resolution TD-OCT was demonstrated with a low crosstalk between adjacent OCT image pixels.[3,11)] However, the fabrication process of crystal fibers is quite complex, and the scanning speeds of TD-OCT systems are slower than of the FD-OCT system.

Recently, technological developments of LED and related phosphors have ushered in a new era in white-light solid-state lighting with low costs and high quantum efficiencies. For the applications of LED on OCT, Fuchi et al. have demonstrated several near-infrared (NIR) sources, including size-dispersed quantum dots LED,[12)] and NIR glass phosphors pumped by 590 nm visible LED.[13,14)] Broadband emissions with 4.6 μm interference signals were observed with high power using NIR glass phosphors and an LED as excitation source.[14)] Thus, finding the framework for linking broadband glass–phosphor-based light source and performing corresponding ultrahigh-resolution optical coherence imaging is an important topic in the following research.

In this paper, the potential utilization of visible LED phosphors as a simple and low-cost light source for ultrahigh-resolution SD-OCT imaging has been evaluated and demonstrated. Excited by a focused 405 nm violet laser beam, broadband spontaneous emissions from LED phosphors were generated and collimated in the visible regime. The broadband light source was centered at 560 nm, with a full width at half maximum (FWHM) of 109 nm, corresponding to a longitudinal resolution of 1.7 μm in air. Then, ultrahigh-resolution 3D SD-OCT imaging was performed with the proposed broadband light source with high spatial coherence.

Figure 1 shows the schematics of the proposed broadband source. In this experiment, a 405 nm diode laser with near TM_{00} spatial distribution, instead of a conventional LED, was selected to improve the spatial coherence of the generated broadband emission. The maximum output power of the 405 nm violet diode laser was 300 mW. The 405 nm laser beam was then focused into LED phosphors dispersed on a microslide glass by means of L_1 (Newport KPX076.AR14) with a focal length of 2.5 cm. The radius of the LED phosphor was 30 μm. The excited broadband emissions from the LED phosphors were then collimated by an achromatic doublet, L_2 (Thorlabs AC127-019-A-ML). Residual 405 nm pump beams were then blocked by a colored glass filter (Thorlabs CG495), and generated broadband spontaneous emissions were then delivered into a home-made ultrahigh-resolution SD-OCT system.

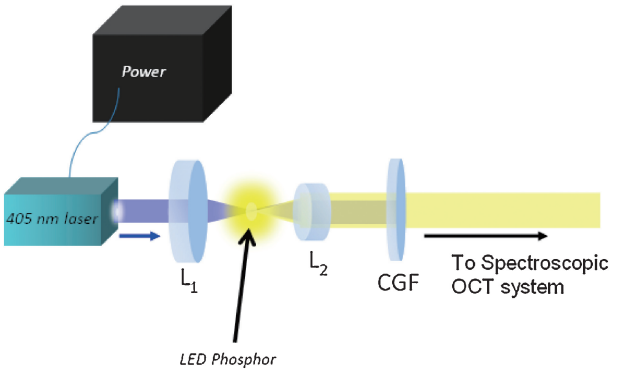

Fig. 1. Setup of phosphor-based light source. L_1 and L_2: collimating and focusing lenses, repectively; CGF: colored glass filter. The LED phosphor was put on the focal spots of L_1 and L_2.

In an ultrahigh-resolution OCT system, the unbalanced dispersion will induce the degradation in the longitudinal resolution. Therefore, the optical path differences induced by the optical components have to be carefully matched between the reference and sample arms.[11] In this experiment, a broadband pellicle beam splitter (Thorlabs BP145B1) with a 2 μm membrane thickness and two identical objectives (Olympus MPlanN 50X/0.75) were carefully put in the SD-OCT system. In the sample arms, a two-axis stepping motor was used to provide the lateral and transverse scanning. Finally, to detect interference spectra, a commercial spectrometer was used and then the interference spectrum was resampled before Fourier transform. The emitted spectrum from the LED phosphor was very clean, thus the pixel crosstalk effect arising from the side lobes was greatly reduced.

To compare the broadband spontaneous emissions from different LED phosphors, three phosphors including green, red, and YAG LED phosphors were utilized in this experiment. The chemical formulas of green, red, and YAG phosphors are $SrGa_2S_4:Eu^{2+}$, $CaS:Eu^{2+}$, and $Y_3Al_5O_{12}:Ce^{3+}$ respectively. Subsequently, three sources were connected to the SD-OCT system to measure the corresponding longitudinal resolutions. Figure 2 shows the results obtained from green, red, and YAG LED phosphors, which were excited by a 405 nm diode laser. In Figs. 2(a), 2(c), and 2(e), the blue and black curves represent the output spectra and

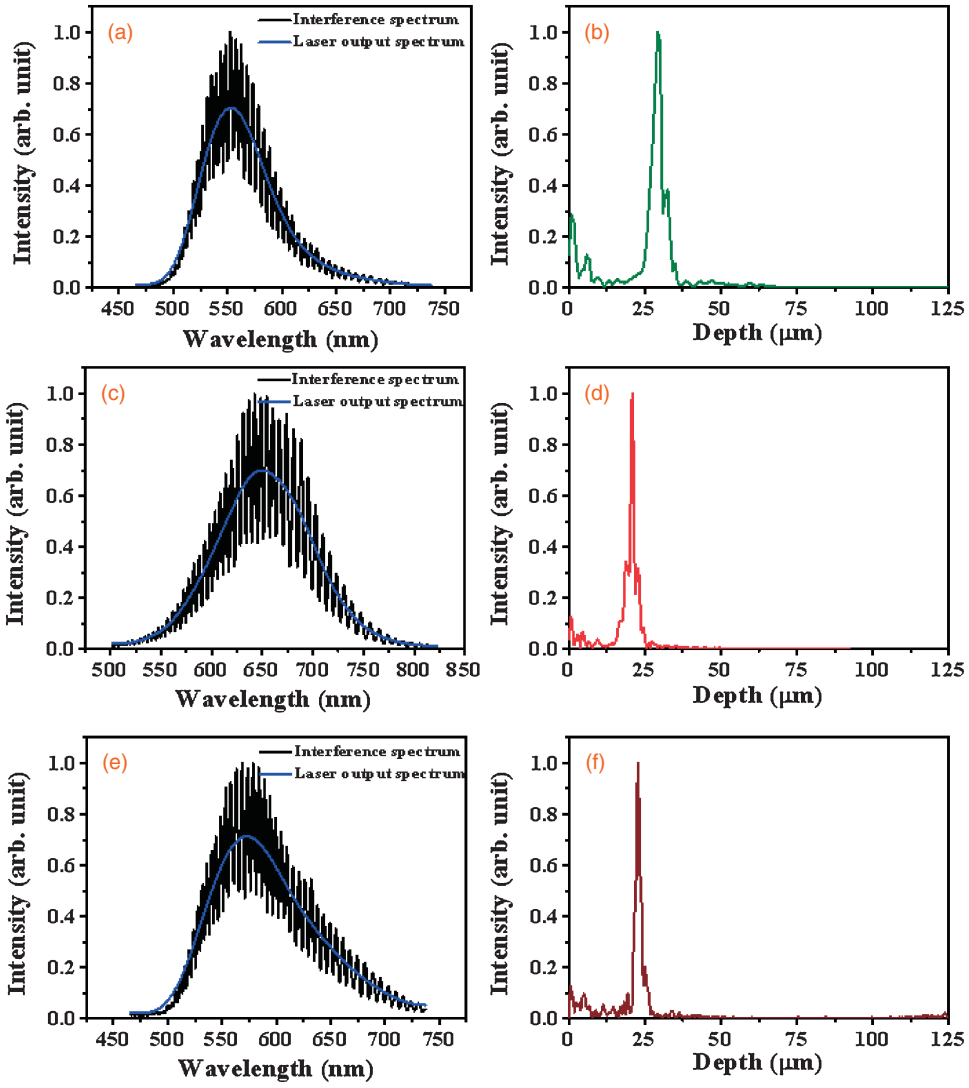

Fig. 2. Source output spectra and interference spectra of green (a), red (c), and YAG (e) phosphor-based light sources. (b), (d), and (f). OCT depth profiles of three phosphor-based light sources. The measured longitudinal resolutions of the three sources are 3.2, 1.9, and 1.7 μm, respectively.

the interference spectra detected by the spectrometer. The central wavelengths of the green, red, and YAG phosphor-based light sources were located at 552, 649, and 572 nm, respectively. The FWHM output spectra of the green, red, and YAG phosphor-based light sources were 73, 109, and 103 nm, respectively.

Assuming that a light source with a Gaussian-like spectrum distribution is used in the OCT system, the longitudinal resolution, Δz, which is related to the spectral range of the light source, $\Delta\lambda$, and the central wavelength of the light source, λ_0, can be expressed as $\Delta z \cong 0.44(\lambda_0^2/\Delta\lambda)$.[1,11] Thus, the calculated theoretical longitudinal resolutions of the OCT system with the three different sources are 1.84, 1.70, and 1.40 μm, respectively. To measure the longitudinal resolution of our SD-OCT system, a partial reflection mirror is used as the sample and the OCT depth profiles of three phosphor-based light sources are shown in Figs. 2(b), 2(d), and 2(f). However, due to the slight dispersion mismatch between the reference and sample arms, the measured longitudinal resolutions of three sources are 3.2, 1.9, and 1.7 μm, as shown in Figs. 2(b), 2(d), and 2(f), respectively. The results show that the measured longitudinal resolution of the YAG phosphor-based source is 1.7 μm in air, corresponding to 1.2 μm in biological tissues. Additionally, the phosphor-based light sources can produce Gaussian-like spectrum shapes, making additional spectrum filters unnecessary for OCT applications.

To demonstrate the feasibility of LED phosphor-based broadband emission with a 300 μW output power as the OCT light sources, the YAG phosphor-based source was chosen and connected to the ultrahigh-resolution SD-OCT system. In this system, the transverse resolution is approximately 2 μm by using a 50× objective lens. With two-axis translational stages, 3D OCT images can be obtained. In our setup, a 3D image consists of $200 \times 200 \times 512$ (x, y, z) voxels, corresponding to a physical size of $200 \times 200 \times 210\,\mu m^3$ (x, y, z). To demonstrate the ability of proving a high longitudinal resolution with the phosphor-based broadband source, a conducting glass was adopted, which has been widely used for display technology, such as a touch panel, and an liquid crystal display (LCD) displayer. In this study, the indium tin oxide (ITO) layer was deposited on a glass substrate with different thicknesses of 5 and 3.5 μm. Figure 3 shows the OCT scanning results of the ITO conducting glass. Figures 3(a) and 3(b) represent the 3D OCT image and the surface plane obtained from the 3D OCT image. In Fig. 3(b), it can be found that a stripe structure shows weaker intensity, resulting from the difference in the thickness of the ITO layer. For further differentiation of the two regions in Fig. 3(b), Figs. 3(c) and 3(d) show the 2D OCT images of locations I and II, indicated by the dashed lines in Fig. 3(b). Here, since the thickness of the glass substrate is approximately 1 mm, the bottom surface of the glass substrate cannot be found in OCT images, limited by the imaging depth of our SD-OCT system. Furthermore, Fig. 3(e) shows the OCT depth profiles of locations A and B. In Fig. 3(e), the first peaks of two curves represent the surface of the ITO conducting layer and the second peaks are induced by the interface of the ITO layer and glass substrate. Hence, from the result, it can be found that the thicknesses

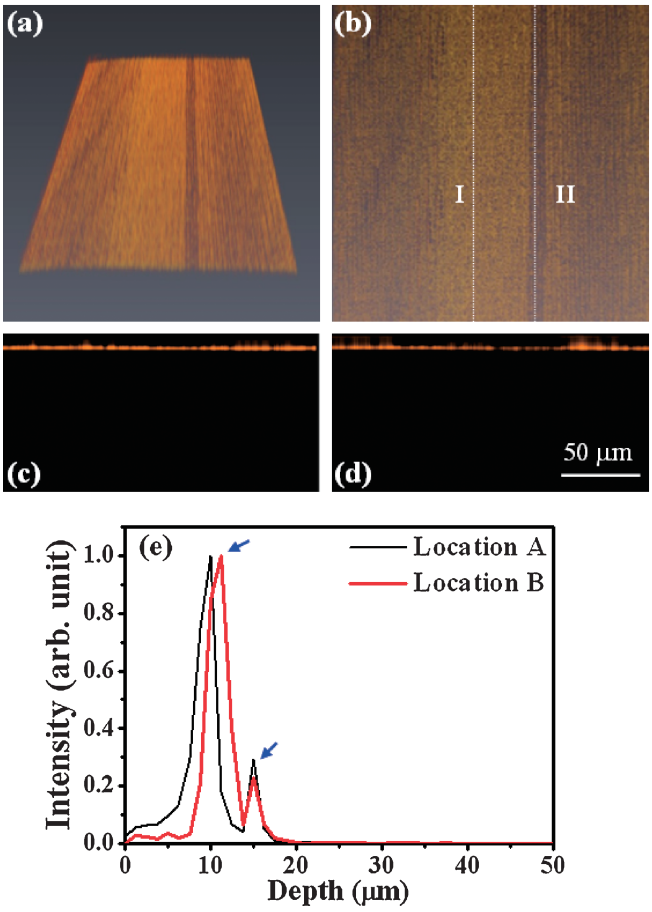

Fig. 3. OCT images of ITO conducting glass. (a) 3D OCT image. (b) Top view of 3D OCT image. (c) and (d) 2D OCT images of locations I and II indicated by dashed lines in (b). (e) OCT depth profiles of locations A and B indicated by dashed lines in (c) and (d), respectively.

of locations A and B can be estimated to be approximately 5.0 and 3.75 μm, respectively. The sensitivity and dynamic range of our OCT system are 92 and 78 dB, respectively, and could be further upgraded by increasing the pump power of the 405 nm diode for increasing the source output power. Limited by the pixel number of the commercial spectrometer that we used (Ocean Optics USB2000), the theoretical imaging depth of the OCT system using the YAG-phosphor light source is approximately 350 μm. The spectrometer can provide a spectral resolution of 0.35 nm, and the detectable spectrum ranges from 200–900 nm. However, the imaging depth can be greatly improved using a specially designed spectrometer. These results demonstrate that it is possible to perform ultrahigh-resolution SD-OCT imaging in the visible region using a phosphor-based broadband light source that is compact, inexpensive, and easy to operate. The demonstrated light source shows great potential for industrial application. Besides, the visible spectral region also covers many absorption bands of numerous biological chromospheres, so the demonstrated ultrahigh resolution source has great potential for spectroscopic OCT. Moreover, because the refractive index in the visible region changes more than that in the NIR regime, the image contrast is stronger in visible region.[15] These optical properties are interesting for biomedical applications, as cell visualization and observation. On the other hand, compared with other

NIR source, this demonstrated broadband visible emission OCT light source and corresponding SD-OCT system are also helpful to clinical retina imaging deep inside the eye with ultrahigh resolution and fast image acquisition.[11)]

In conclusion, simple, low-cost, and broadband sources in the visible spectrum range were proposed and demonstrated by using green, red, and YAG LED phosphors pumped by a violet laser diode. For OCT applications, the corresponding longitudinal resolutions of green, red, and YAG LED phosphor-based broadband sources are 3.2, 1.9, and 1.7 μm, respectively. Based on the broadband source, an ultrahigh-resolution 3D SD-OCT imaging was performed for the first time and used for scanning the conducting glass. The results show that the thickness of the conducting layer can be obtained using the phosphor-based OCT system. The demonstrated ultra-broadband light source, which is simple in configuration and cost-effective, shows great potential for future OCT applications, including biological research cells structures, clinical research of eyes and industrial inspection.

Acknowledgments The authors acknowledge the scientific discussions with Professor C. K. Sun of National Taiwan University. This research was supported in part by the National Science Council of Taiwan, R.O.C. (NSC 100-2221-E-009-092-MY3) and the Chi-Mei Medical Center, Tainan.

1) D. Huang, E. A. Swanson, C. P. Lin, J. S. Schuman, W. G. Stinson, W. Chang, M. R. Hee, T. Flotte, K. Gregory, C. A. Puliafito, and J. G. Fujimoto: Science **254** (1991) 1178.
2) M. Wojtkowski: Appl. Opt. **49** (2010) D30.
3) Y.-S. Lin, T.-C. Cheng, C.-C. Tsai, K.-Y. Hsu, D.-Y. Jheng, C.-Y. Lo, P.-H. S. Yeh, and S.-L. Huang: IEEE Photonics Technol. Lett. **22** (2010) 1494.
4) T.-H. Tsai, B. Potsaid, Y. K. Tao, V. Jayaraman, J. Jiang, P. J. S. Heim, M. F. Kraus, C. Zhou, J. Hornegger, H. Mashimo, A. E. Cable, and J. G. Fujimoto: Biomed. Opt. Express **4** (2013) 1119.
5) D. C. Adler, R. Huber, and J. G. Fujimoto: Opt. Lett. **32** (2007) 626.
6) R. Leitgeb, C. K. Hitzenberger, and A. F. Fercher: Opt. Express **11** (2003) 889.
7) H. Lim, Y. Jiang, Y. Wang, Y.-C. Huang, Z. Chen, and F. W. Wise: Opt. Lett. **30** (2005) 1171.
8) K. Q. Kieu, J. Klein, A. Evans, J. K. Barton, and N. Peyghambarian: J. Biomed. Opt. **16** (2011) 106004.
9) T. H. Ko, D. C. Adler, J. G. Fujimoto, D. Mamedov, V. Prokhorov, V. Shidlovski, and S. Yakubovich: Opt. Express **12** (2004) 2112.
10) G. Moneron, A. C. Boccara, and A. Dubois: Opt. Lett. **30** (2005) 1351.
11) C.-C. Tsai, T.-H. Chen, Y.-S. Lin, Y.-T. Wang, W. Chang, K.-Y. Hsu, Y.-H. Chang, P.-K. Hsu, D.-Y. Jheng, K.-Y. Huang, E. Sun, and S.-L. Huang: Opt. Lett. **35** (2010) 811.
12) S. Fuchi, K. Tani, T. Arai, S. Kamiyama, and Y. Takeda: Phys. Status Solidi C **9** (2012) 2348.
13) S. Fuchi, A. Sakano, R. Mizutani, and Y. Takeda: Appl. Phys. B **105** (2011) 877.
14) S. Fuchi, A. Sakano, R. Mizutani, and Y. Takeda: Appl. Phys. Express **2** (2009) 032102.
15) W. Drexler and J. G. Fujimoto: *Optical Coherence Tomography Technology and Applications* (Springer, New York, 2008) 1st ed., p. 271.